# Model-Based Position Tracking Control for a 6-dof Electrohydraulic Stewart Platform

Ioannis Davliakos and Evangelos Papadopoulos, *Senior Member, IEEE*

*Abstract*— **In this paper, a position tracking controller for a six-degree-of-freedom (dof) electrohydraulic Stewart platform mechanism is developed that includes a fast inner model-based force tracking loop. A full rigid body model and an electrohydraulic actuator model, including friction and servovalve characteristics are employed and described by a set of integrated system equations. The control analysis is based on a nonlinear input-output linearization control approach. The developed control law also contains a PD part, responsible for the exponential convergence of the tracking error to zero. Simulations with typical desired trajectories are presented and a good tracking performance is obtained.**

## I. Introduction

The original six-Degree-of-Freedom (dof) Stewart-Gough platform was developed in 1954 [1], [2]. In 1965, the prototype parallel mechanism was used as a 6-dof motion platform for a flight simulator [3]. Since then, a number of studies of this mechanism and its variations have been published, see for example [4]. The mechanism can be driven electrically or electrohydraulically. The kinematics and dynamics of the Stewart platform have been studied by many researchers [5]–[8]. However, actuation dynamics have not been considered. Although electrohydraulic Stewart platforms have been used extensively, little published work on their full dynamics including actuation and control, exists.

Hydraulics science combined with controls, has given a new thrust to hydraulics applications. The main reasons for which hydraulics are preferred to electromechanical drives in a number of industrial and mobile applications, include their ability to produce large forces at high speeds, their high durability and stiffness, and their rapid response [9], [10]. Hydraulic regimes differ from electromechanical ones, in that the force or torque output is not proportional to actuator current and therefore, hydraulic actuators cannot be modeled as force/ torque sources, but as controlled impedances. As a result, robot or flight simulator controllers that require force sources, cannot be used here.

Control techniques are used to compensate for the nonlinearities of electrohydraulic servosystems. Nonlinear adaptive control techniques for hydraulic servosystems have been proposed by researchers employing linearization, [11], or backstepping, [12], approaches. A robust force controller design based on the nonlinear Quantitative Feedback Theory, has been implemented on an industrial hydraulic actuator, taking into account system and environmental uncertainties [13].

Most of the previous work associated with force/ pressure control has focused on electrohydraulic servo-actuators and has been developed based on Lyapunov analysis [14]-[16]. A model based controller of hydraulically actuated manipulators has been studied, but the feedforward controller terms were calculated using desired and not actual positions, [17]. Early efforts on a model-based force/ motion control analysis for a 1-dof system has been developed with satisfactory tracking response, [18].

In this paper, a model-based position tracking controller is developed for a 6 dof electrohydraulic Stewart platform with symmetric joint locations, using a fast inner force loop. Dynamic models are used that describe the rigid body motion of the Stewart platform and its hydraulic actuation system. In contrast to other approaches, here, servovalve models and friction are included in the model. The developed control scheme employs rigid body and actuation dynamics and yields the servovalve input current vector, in analytical form. A model-based force controller is developed, which is augmented by a PD part, responsible for the exponential convergence of the tracking error to zero. The performance of the developed controller is illustrated using typical trajectories. The proposed methodology can be extended to electrohydraulic serial or closed-chain manipulators and simulators.

## II. Electrohydraulic Stewart Platform Modeling

### A. Mechanical Dynamics

In this section, the dynamic model of a 6-dof electrohydraulic Stewart platform servomechanism [3] is developed. This is a six dof closed kinematic chain mechanism consisting of a fixed base and a moving platform with six

Manuscript received February 1, 2007.

I. Davliakos is with the National Technical University of Athens, Greece (e-mail: gdavliak@central.ntua.gr).

E. Papadopoulos is with the National Technical University of Athens (NTUA), Greece (corresponding author, phone: +(30) 210-772-1440; fax: +(30) 210-772-1455; e-mail: egpapado@central.ntua.gr).

Support of this work by the Hellenic General Secretariat for Research and Technology (EPAN M. 4.3.6.1), is acknowledged.

linear actuators supporting it. The mechanism is illustrated schematically in Fig. 1.

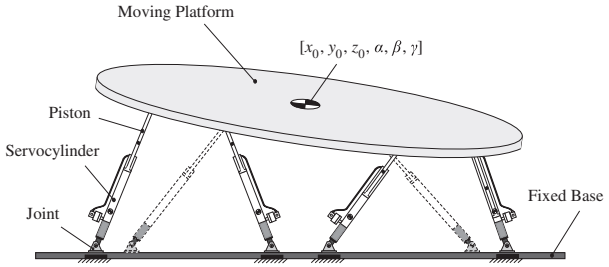


Fig. 1. Schematic view of a six-dof Stewart Platform.

The equation of motion for the Stewart mechanism is derived applying a Lagrangian formulation and is written as,

$$\mathbf{M}(\mathbf{q})\ddot{\mathbf{q}} + \mathbf{V}(\mathbf{q},\dot{\mathbf{q}}) + \mathbf{G}(\mathbf{q}) + \mathbf{F}_{fr}(\dot{\mathbf{q}}) = \boldsymbol{\tau} \tag{1}$$

where $\mathbf{q} = (x_0, y_0, z_0, \alpha, \beta, \gamma)^{\mathrm{T}}$ is the $6\times1$ vector of the platform generalized coordinates, see Fig. 1, $x_0$, $y_0$, $z_0$, are the platform center of mass Cartesian coordinates, $\alpha$, $\beta$, $\gamma$ are the platform Euler angles, $\mathbf{M}(\mathbf{q})$ is the $6\times6$ positive definite mass matrix of the system, the $6\times1$ vector $\mathbf{V}(\mathbf{q},\dot{\mathbf{q}})$ represents forces/ torques arising from centrifugal and Coriolis forces, the $6\times1$ vector $\mathbf{G}(\mathbf{q})$ represents torques due to gravity, $\mathbf{F}_{fr}(\dot{\mathbf{q}})$ is the $6\times1$ vector of the forces/ torques due to friction, and $\boldsymbol{\tau}$ is the $6\times1$ vector of the generalized applied forces.

Equation (1) can be further extended using the transformation between mechanism actuator forces and the generalized applied forces, [4], which is given by,

$$\boldsymbol{\tau} = \mathbf{J}^{\mathrm{T}}\mathbf{F}_p \tag{2}$$

where $\mathbf{J}$ is the Jacobian $6\times6$ matrix of the system, and $\mathbf{F}_p$ is a $6\times1$ vector representing actuator forces given by,

$$\mathbf{F}_p = (F_{p,1}, F_{p,2}, ..., F_{p,6})^{\mathrm{T}} \tag{3}$$

where $F_{p,j}$, $j = 1,2,...,6$ are individual hydraulic forces acting on actuator pistons.

Further, using mechanism differential kinematics the platform Cartesian motion described by (1) can be transformed in its joint space and written as,

$$\mathbf{M}^*(\mathbf{q})\ddot{\boldsymbol{\ell}} + \mathbf{V}^*(\mathbf{q},\dot{\mathbf{q}}) + \mathbf{G}^*(\mathbf{q}) + \mathbf{F}^*_{fr}(\dot{\boldsymbol{\ell}}) = \mathbf{F}_p \tag{4}$$

where $\boldsymbol{\ell} = (\ell_1, \ell_2, ..., \ell_6)^{\mathrm{T}}$ is the $6\times1$ vector of the mechanism actuator lengths, $\mathbf{M}^*(\mathbf{q})$ is a $6\times6$ positive definite mass matrix, $\mathbf{V}^*(\mathbf{q},\dot{\mathbf{q}})$ is a $6\times1$ vector that contains the centrifugal and Coriolis forces, $\mathbf{G}^*(\mathbf{q})$ is a $6\times1$ gravity forces vector, and $\mathbf{F}^*_{fr}(\dot{\boldsymbol{\ell}})$ is a $6\times1$ vector that contains joint space frictional forces. The terms $\mathbf{M}^*(\mathbf{q})$, $\mathbf{V}^*(\mathbf{q},\dot{\mathbf{q}})$ and $\mathbf{G}^*(\mathbf{q})$ are given, respectively by,

$$\mathbf{M}^*(\mathbf{q}) = [\mathbf{J}(\mathbf{q})^{\mathrm{T}}]^{-1}\,\mathbf{M}(\mathbf{q})\,\mathbf{J}(\mathbf{q})^{-1} \tag{5a}$$

$$\mathbf{V}^*(\mathbf{q},\dot{\mathbf{q}}) = [\mathbf{J}(\mathbf{q})^{\mathrm{T}}]^{-1}[\mathbf{V}(\mathbf{q},\dot{\mathbf{q}}) - \mathbf{M}(\mathbf{q})\,\dot{\mathbf{J}}(\mathbf{q},\dot{\mathbf{q}})\cdot\dot{\mathbf{q}}] \tag{5b}$$

$$\mathbf{G}^*(\mathbf{q}) = [\mathbf{J}(\mathbf{q})^{\mathrm{T}}]^{-1}\mathbf{G}(\mathbf{q}) \tag{5c}$$

The friction vector $\mathbf{F}^*_{fr}(\dot{\boldsymbol{\ell}})$ can be written as,

$$\mathbf{F}^*_{fr}(\dot{\boldsymbol{\ell}}) = \mathbf{F}^*_v(\dot{\boldsymbol{\ell}}) + \mathbf{F}^*_C(\dot{\boldsymbol{\ell}}) + \mathbf{F}^*_s \tag{6}$$

where $\mathbf{F}^*_v(\dot{\boldsymbol{\ell}})$, $\mathbf{F}^*_C(\dot{\boldsymbol{\ell}})$ and $\mathbf{F}^*_s$ are the viscous, Coulomb and static friction vector respectively, with elements,

$$F^*_{v,j}(\dot{\ell}_j) = \begin{cases} b_j\dot{\ell}_j, & \dot{\ell}_j \neq 0, \quad j = 1,2,...,6 \\ 0, & \dot{\ell}_j = 0, \quad j = 1,2,...,6 \end{cases} \tag{7a}$$

$$F^*_{C,j}(\dot{\ell}_j) = \begin{cases} F^*_{C0,j}\,sign(\dot{\ell}_j), & \dot{\ell}_j \neq 0, \quad j = 1,2,...,6 \\ 0, & \dot{\ell}_j = 0, \quad j = 1,2,...,6 \end{cases} \tag{7b}$$

$$F^*_{s,j} = \begin{cases} F_{ext,j}, & |F_{ext,j}| < F^*_{s0,j},\ \dot{\ell}_j = 0,\ \ddot{\ell}_j = 0, \quad j=1,...,6 \\ F^*_{s0,j}\,sign(F_{ext,j}), & |F_{ext,j}| > F^*_{s0,j},\ \dot{\ell}_j = 0,\ \ddot{\ell}_j \neq 0, \quad j=1,...,6 \\ 0, & \dot{\ell}_j \neq 0, \quad j=1,...,6 \end{cases} \tag{7c}$$

where $b_j$ is the j[th] parameter for viscous friction element, $F^*_{C0,j}$ is the j[th] parameter for Coulomb friction element, $F_{ext,j}$ is the j[th] external force element, $F^*_{s0,j}$ is the j[th] breakaway force element.

### *B. Hydraulic Dynamics*

The electrohydraulic actuation Stewart servosystem consists of pistons, servovalves, controllers, sensors and a hydraulic power supply. Next, hydraulic models of electrohydraulic servosystem major components are introduced.

The hydraulic supply includes a pump that is usually constant pressure piston pump, driven by an induction electric motor. Therefore, the pump is modelled as a constant pressure source. Further, it may include accumulators for filtering pressure pulsations from the pump, but also for allowing the use of smaller rating pumps by providing additional flow when needed. Such an accumulator is modelled as a hydraulic capacitor, [19].

A single rod hydraulic servocylinder is illustrated schematically in Fig. 2. The equations relating mechanical to hydraulic variables are described by,

$$Q_1 = A_1\dot{\ell} + C_1\dot{p}_1 + G_{p,in}(p_1 - p_2) \tag{8a}$$

$$Q_2 = A_2\dot{\ell} - C_2\dot{p}_2 + G_{p,in}(p_1 - p_2) \tag{8b}$$

$$A_1 p_1 - A_2 p_2 = F_p \tag{8c}$$

$$F_{net} = F_p - F_{fr,p} \tag{8d}$$

where $Q_1$, $Q_2$ are the flows through the two cylinder chamber ports, $p_1$, $p_2$ are the chamber pressures, $A_1$ is the piston side area, $A_2$ is the rod side area, $C_1$, $C_2$ are the fluid capacitances of the cylinder chambers, $G_{p,in}$ represents the cylinder internal leakage conductance, $\ell$ is shown in Fig. 2, $F_p$ is the hydraulic force, $F_{fr,p}$ is the actuator friction force, and $F_{net}$ is the net actuator output

force. In the case of a hydraulic cylinder with a double rod, the two areas $A_1$ and $A_2$ are equal and therefore, (8) are simplified.

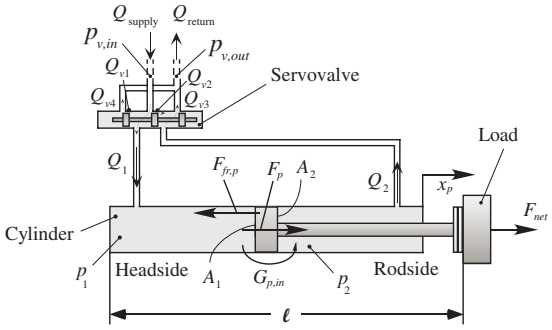


Fig. 2. Schematic model of a hydraulic servoactuator.

Control of a hydraulic system is achieved through the use of servovalves, see Fig. 3(a). Only the resistive effect of a valve is considered here, since their natural frequency is much higher than that of the mechanical load. It is also assumed that the geometry of the valve is ideal, e.g. the valve has sharp edges and zero cross leakage, [20], [21].

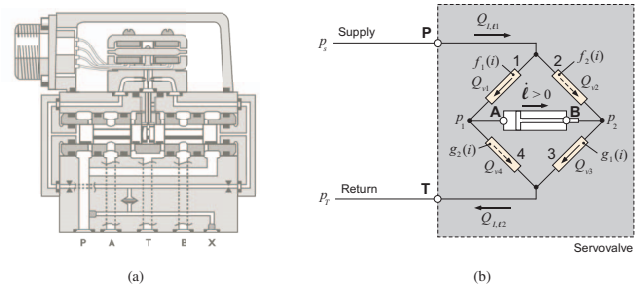


Fig. 3. (a) A drawing of a real servovalve, (b) Schematic model of servovalve.

A typical hydraulic servovalve consists of four symmetric and matched servovalve orifices making up flow paths through four nonlinear resistors, modulated by the input voltage, see Fig. 3(a). Thereby, the servovalve is modeled as the hydraulic equivalent of a Wheatstone bridge, see Fig. 3(b). When the servovalve input current is positive, $i>0$, flow passes through the orifices 1 and 3 (path $P-A-B-T$), and flow leakages exist in the valve orifices 2 and 4. Similarly, when the servovalve input current is negative, $i<0$, flow passes through the path $P-A-B-T$, and flow leakages exist in the valve orifices 1 and 3. This model is described by,

$$Q_{v1}=f_1(i,C_d,\rho)\sqrt{p_{v,in}-p_1}\equiv C_{G_1}\sqrt{p_{v,in}-p_1} \tag{9a}$$

$$Q_{v2}=f_2(i,C_d,\rho)\sqrt{p_{v,in}-p_2}\equiv C_{G_2}\sqrt{p_{v,in}-p_2} \tag{9b}$$

$$Q_{v3}=g_1(i,C_d,\rho)\sqrt{p_2-p_{v,out}}\equiv C_{G_3}\sqrt{p_2-p_{v,out}} \tag{9c}$$

$$Q_{v4}=g_2(i,C_d,\rho)\sqrt{p_1-p_{v,out}}\equiv C_{G_4}\sqrt{p_1-p_{v,out}} \tag{9d}$$

where $Q_{v1}$, $Q_{v2}$, $Q_{v3}$ and $Q_{v4}$ are the servovalve flows through the orifices 1, 2, 3 and 4, respectively, $p_{v,in}$ and $p_{v,out}$ are the input and output servovalve pressure of the servosystem, correspondingly, $i$ is the servovalve motor current (control command), and $f_1(i,C_d,\rho)$, $f_2(i,C_d,\rho)$, $g_1(i,C_d,\rho)$ and $g_2(i,C_d,\rho)$ are nonlinear functions in the servovalve motor current, the discharge coefficient $C_d$ and the mass density of the fluid, $\rho$. In general, the discharge coefficient is a function of the *Reynolds* number and valve geometry. However, fluid density and Reynolds dependencies are weak for turbulent flow and therefore only the current dependency is significant here, [9]; therefore, the functions $f_1(i,C_d,\rho)$, $f_2(i,C_d,\rho)$, $g_1(i,C_d,\rho)$, $g_2(i,C_d,\rho)$ are reduced to $f_1(i)$, $f_2(i)$, $g_1(i)$, $g_2(i)$, correspondingly. Because of servovalve symmetry, the current functions are described by the following statements,

- If $i>0$, the main flow path passes through the orifices 1 and 3, see Fig. 3(b), and the servovalve functions are given by,

$$f_1(i)=g_1(i)\equiv C_{G_{sv,main}}(i),\ \ f_2(i)=g_2(i)\equiv C_{G_{sv,leak}}(i) \tag{10}$$

- If $i<0$, the main flow path passes through the orifices 2 and 4, see Fig. 3(b), and the servovalve functions are given by,

$$f_2(i)=g_2(i)\equiv C_{G_{sv,main}}(-i),\ \ f_1(i)=g_1(i)\equiv C_{G_{sv,leak}}(-i) \tag{11}$$

where $C_{G_{sv,main}}$ and $C_{G_{sv,leak}}$ represent current functions with respect to the main and leakage flow of the servovalve, respectively. A good approximation of these functions is as follows,

$$C_{G_{sv,main}}(i)=\begin{cases}K_{1,main}\,i+K_{0,main}, & |i|>i_{0,main}\\ k_{2,main}\,i|i|+k_{1,main}\,i+k_0, & |i|<i_{0,main}\end{cases} \tag{12a}$$

$$C_{G_{sv,leak}}(i)=\begin{cases}K_{0,leak}, & |i|>i_{0,leak}\\ k_{3,leak}\,i^3+k_{2,leak}\,i|i|+k_{1,leak}\,i+k_0, & |i|<i_{0,leak}\end{cases} \tag{12b}$$

where the coefficients $K_{1,main}$, $K_{0,main}$ and $K_{0,leak}$ are positive constants parameters, the coefficients $k_{1,main}$, $k_{2,main}$, $k_{1,leak}$, $k_{2,leak}$, $k_{3,leak}$ and $k_0$ are constants parameters, and $i_{0,main}$, $i_{0,leak}$ are characteristic values of the servovalve current, which correspond to the main and leakage valve path, respectively.

If leakage flows and cylinder chamber compressibility are neglected, the flows through the orifices of the servovalve described by (9a,c) are equal to the flows through cylinder chamber ports, see (8a,b), and are written as,

$$Q_{v1}=Q_1=A_1\dot{\ell}+C_1\dot{p}_1+G_{p,in}(p_1-p_2) \tag{13a}$$

$$Q_{v3}=Q_2=A_2\dot{\ell}-C_2\dot{p}_2+G_{p,in}(p_1-p_2) \tag{13b}$$

Hydraulic hoses of the 6-dof electrohydraulic servosystem are modeled as compressible hydraulic lines, [19]. The equations that describe the hose dynamics are given by,

$$p_{l,in} - p_{l,m} = R\,Q_{l,in} \tag{14a}$$

$$\dot{Q}_{l,out} = (p_{l,m} - p_{l,out}) \cdot I^{-1} \tag{14b}$$

$$\dot{p}_{l,m} = (Q_{l,in} - Q_{l,out}) \cdot C^{-1} \tag{14c}$$

where $p_{l,in}$, $p_{l,out}$, and $p_{l,m}$ are hose pressures at its input, output and a middle point respectively, $Q_{l,in}$, $Q_{l,out}$ are the flows through the hose at its input and output correspondingly. The parameters $R$, $I$, $C$ correspond to hose resistance, inertance and capacitance, respectively.

### C. Integrated System Equations

The hydraulic and load dynamic response can be described by a set of integrated system equations derived using a systems approach, such as the Linear Graph [20] or Bond Graph methods [22]. To this end, one needs to provide expressions transforming pressure differences to forces, see (9c), and velocities to flows, see (8a,b).

Here, the Linear Graph method is used. The application of continuity and compatibility laws, along with individual elements equations, leads in a set of forty-two non-linear first order differential equations, as follows,

$$\dot{p}_{1,j} = [Q_{I,\ell 1} - Q_{v2}(i) - Q_{v4}(i) - G_{p,in}\cdot(p_1 - p_2) - A_1 v]\cdot C_1^{-1}\big|_j, \quad j=1,2,...,6 \tag{15a}$$

$$\dot{p}_{2,j} = [Q_{v2}(i) + Q_{v4}(i) - Q_{I,\ell 2} + G_{p,in}\cdot(p_1 - p_2) + A_2 v]\cdot C_2^{-1}\big|_j, \quad j=1,2,...,6 \tag{15b}$$

$$\dot{p}_{C,\ell 1,j} = [(p_s - p_{C,\ell 1})R_{\ell 1}^{-1} - Q_{I,\ell 1}]\cdot C_{\ell 1}^{-1}\big|_j, \quad j=1,2,...,6 \tag{15c}$$

$$\dot{p}_{C,\ell 2,j} = [Q_{I,\ell 2} - (p_{C,\ell 2} - p_T)R_{\ell 2}^{-1}]\cdot C_{\ell 2}^{-1}\big|_j, \quad j=1,2,...,6 \tag{15d}$$

$$\dot{Q}_{I,\ell 1,j} = [p_{C,\ell 1} - p_1 - \Delta p_{G_1}(i)]\cdot I_{\ell 1}^{-1}\big|_j, \quad j=1,2,...,6 \tag{15e}$$

$$\dot{Q}_{I,\ell 2,j} = [p_2 - p_{C,\ell 2} - \Delta p_{G_3}(i)]\cdot I_{\ell 2}^{-1}\big|_j, \quad j=1,2,...,6 \tag{15f}$$

$$\dot{v}_j = [\mathbf{m}_-^*]\big|_j \cdot (\mathbf{F}_p - \mathbf{V}^* - \mathbf{G}^* - \mathbf{F}_{fr}^*), \quad j=1,2,...,6 \tag{15g}$$

where $Q_{I,\ell 1,j}$, $Q_{I,\ell 2,j}$ are the j$^{th}$ flows in the j$^{th}$ hydraulic pressure and return line correspondingly, $p_s$, $p_T$ are the power supply and return pressure of the servosystem, respectively, $p_{C,\ell 1,j}$, $p_{C,\ell 2,j}$ are correspondingly the j$^{th}$ pressures of j$^{th}$ hydraulic power and return line regarding with the lines' capacitances, $I_{\ell 1,j}$, $R_{\ell 1,j}$, $C_{\ell 1,j}$ are the j$^{th}$ inertance, resistance and capacitance of j$^{th}$ hydraulic power line respectively, $I_{\ell 2,j}$, $R_{\ell 2,j}$, $C_{\ell 2,j}$ are the j$^{th}$ inertance, resistance and capacitance of j$^{th}$ hydraulic return line respectively, $v_j = \dot{\ell}_j$ is the velocity of the j$^{th}$ piston, which is obtained by (4), $[\mathbf{m}_-^*]\big|_j$ is a $1\times 6$ row-matrix which corresponds to the j$^{th}$ line of the matrix $(\mathbf{M}^*)^{-1}$. The terms $\Delta p_{G_1}(i)\big|_j$, $\Delta p_{G_3}(i)\big|_j$ are the j$^{th}$ pressure drops of the j$^{th}$ servovalve orifices 1 and 3 respectively, which are determined using the flow continuity laws, along with actuator and servovalve elements equations, and given by,

$$\Delta p_{G_1}(i)\big|_j = \{[C_{G_1}^2(i) - C_{G_2}^2(i)]^{-1}\cdot[Q_{I,\ell 1}C_{G_1}(i) - C_{G_2}(i)\cdot\sqrt{Q_{I,\ell 1}^2 + [C_{G_1}^2(i) - C_{G_2}^2(i)]\cdot(p_1 - p_2)}]\}^2\big|_j, \quad j=1,2,...,6 \tag{16a}$$

$$\Delta p_{G_3}(i)\big|_j = \{[C_{G_3}^2(i) - C_{G_4}^2(i)]^{-1}\cdot[Q_{I,\ell 2}C_{G_3}(i) - C_{G_4}(i)\cdot\sqrt{Q_{I,\ell 2}^2 + [C_{G_3}^2(i) - C_{G_4}^2(i)]\cdot(p_1 - p_2)}]\}^2\big|_j, \quad j=1,2,...,6 \tag{16b}$$

where $C_{G_1}(i)\big|_j$, $C_{G_2}(i)\big|_j$, $C_{G_3}(i)\big|_j$, $C_{G_4}(i)\big|_j$ were defined in (9)–(12).

Further, using the flow continuity laws, along with hydraulic lines and servovalve elements equations, the flows $Q_{v2,j}(i)$ and $Q_{v4,j}(i)$ in (15a,b), are determined by,

$$Q_{v2,j}(i) = [Q_{I,\ell 1} - C_{G_1}(i)\sqrt{\Delta p_{G_1}(i)}]\big|_j, \quad j=1,2,...,6 \tag{17a}$$

$$Q_{v4,j}(i) = [Q_{I,\ell 2} - C_{G_3}(i)\sqrt{\Delta p_{G_3}(i)}]\big|_j, \quad j=1,2,...,6 \tag{17b}$$

## III. Controller Design

In this section, a model-based nested position tracking controller using a fast inner force loop is developed, which is augmented by a PD part, responsible for the exponential convergence of the tracking error to zero.

In electromechanical systems, the force acting on moving masses is proportional to actuator current. This simplifies their control laws and allows one to achieve second order error dynamics converging exponentially to zero. However, a simple relationship between force and current does not exist in electrohydraulic systems. Despite of this, we are interested in studying whether such a system can be described by error dynamics such as,

$$\ddot{\mathbf{e}} + \mathbf{K}_v\dot{\mathbf{e}} + \mathbf{K}_p\mathbf{e} = \mathbf{0} \tag{18}$$

where $\mathbf{K}_p$ and $\mathbf{K}_v$ are $6\times 6$ diagonal matrices, which represent the control gains of the system, and $\mathbf{e} = \boldsymbol{\ell}_{des} - \boldsymbol{\ell}$ is the $6\times 1$ position error vector.

Since Eq. (18) is a second-order differential equation, matrix factors $\mathbf{K}_p$ and $\mathbf{K}_v$ can be written in terms of the closed-loop natural frequency $\omega_j$ and damping $\zeta_j$, $j=1,2,...,6$, for all six linear actuators, as,

$$\mathbf{K}_p = \mathrm{diag}\{\omega_1^2,...,\omega_6^2\},\ \mathbf{K}_v = \mathrm{diag}\{2\zeta_1\omega_1,...,2\zeta_6\omega_6\} \tag{19}$$

Employing a pole placement technique, one can guarantee system stability as well as its transient response. Therefore, system closed-loop natural frequency and damping can be selected so that the poles lie in a desirable area of the left half complex plane. Equation (19) yields then the necessary feedback loop gains.

For control purposes, determination of the six forces acting on the platform is considered next. These are the net

platform actuation forces that can be measured via force sensors, e.g. [23], or computed by,

$$\mathbf{F}_{net} = \mathbf{M}_{pl}(\mathbf{q})\ddot{\boldsymbol{\ell}} + \mathbf{V}_{pl}(\mathbf{q},\dot{\mathbf{q}}) + \mathbf{G}_{pl}(\mathbf{q}) \tag{20}$$

where $\mathbf{M}_{pl}$ is the $6\times6$ positive definite mass matrix of the platform, $\mathbf{V}_{pl}$ represents forces/ torques arising from centrifugal and Coriolis forces on the platform, and $\mathbf{G}_{pl}$ represents platform torques due to gravity.

Assuming that (18) have been achieved, this equation is solved for $\ddot{\boldsymbol{\ell}}$ which is then substituted in (20). The result is a force that must be applied by the pistons, so that the error of the load motion is governed by (18). Therefore, the desired actuator forces are given by,

$$\begin{aligned}\mathbf{F}_{net,des} = \mathbf{M}_{pl}(\mathbf{q})\cdot[\ddot{\boldsymbol{\ell}}_{des} + \mathbf{K}_v(\dot{\boldsymbol{\ell}}_{des} - \dot{\boldsymbol{\ell}}) + \mathbf{K}_p(\boldsymbol{\ell}_{des} - \boldsymbol{\ell})] + \\ \mathbf{V}_{pl}(\mathbf{q},\dot{\mathbf{q}}) + \mathbf{G}_{pl}(\mathbf{q})\end{aligned} \tag{21}$$

To generate a relationship between force and current, (21) is differentiated up to the point that the input does not explicitly appear. Differentiating once, (21) yields,

$$\dot{\mathbf{F}}_{net} = \dot{\mathbf{F}}_{net}(\boldsymbol{\ell},\dot{\boldsymbol{\ell}},\dot{\mathbf{v}},\ddot{\mathbf{v}}) \tag{22}$$

where $\mathbf{v} = \dot{\boldsymbol{\ell}}$ is the $6\times1$ linear velocity piston vector.

Differentiating the piston acceleration, (15g), yields,

$$\ddot{\mathbf{v}} = \ddot{\mathbf{v}}(\boldsymbol{\ell},\dot{\boldsymbol{\ell}},\mathbf{p}_1,\mathbf{p}_2) \tag{23}$$

where $\mathbf{p}_1$ and $\mathbf{p}_2$ are the $6\times1$ chamber pressure vectors of the servoactuators.

Taking into account (15a-g), (22) takes the form,

$$\dot{\mathbf{F}}_{net} = \dot{\mathbf{F}}_{net}(\boldsymbol{\ell},\dot{\boldsymbol{\ell}},\mathbf{p}_1,\mathbf{p}_2) \tag{24}$$

Further, substituting (9)-(12) into (24), yields,

$$\dot{\mathbf{F}}_{net} = \begin{cases} \hbar_{11}(\boldsymbol{\ell},\dot{\boldsymbol{\ell}},\mathbf{p}_1,\mathbf{p}_2)\cdot\mathbf{i} + \hbar_{10}(\boldsymbol{\ell},\dot{\boldsymbol{\ell}},\mathbf{p}_1,\mathbf{p}_2), \\ \qquad |i_j| > i_{0,main,j},\ j=1,...,6 \\ \hbar_{22}(\boldsymbol{\ell},\dot{\boldsymbol{\ell}},\mathbf{p}_1,\mathbf{p}_2)\cdot \mathrm{diag}\{|i_j|\}\cdot\mathbf{i} + \hbar_{21}(\boldsymbol{\ell},\dot{\boldsymbol{\ell}},\mathbf{p}_1,\mathbf{p}_2)\cdot\mathbf{i} \\ \quad + \hbar_{20}(\boldsymbol{\ell},\dot{\boldsymbol{\ell}},\mathbf{p}_1,\mathbf{p}_2),\ |i_j| < i_{0,main,j},\ j=1,...,6 \end{cases} \tag{25}$$

where $\mathbf{i}$ is the $6\times1$ servovalve current vector, $\hbar_{11}$, $\hbar_{22}$, $\hbar_{21}$, and $\hbar_{10}$, $\hbar_{20}$ are respectively $6\times6$ diagonal nonlinear matrices and $6\times1$ vector functions with elements the system state variables.

Equation (25) shows that one can find a relationship between the current and the derivative of the force and not the force itself, as in electric actuators. Also, (25) suggests that one can design a controller that will allow the output force to converge to the desired one according to the following first order error equation,

$$\dot{\mathbf{e}}_f + \mathbf{K}_f\mathbf{e}_f = \mathbf{0} \tag{26}$$

where the $6\times6$ diagonal matrix $\mathbf{K}_f$ is the force gain and $\mathbf{e}_f = \mathbf{F}_{net,des} - \mathbf{F}_{net}$ is the $6\times1$ force error vector.

Assuming that (26) have been achieved, this equation is solved for $\dot{\mathbf{F}}_{net}$, which is then substituted in (25). Next, solving (25) for the servovalve current vector $\mathbf{i}$, the control law is obtained as,

$$\mathbf{i} = \mathbf{i}(\boldsymbol{\ell},\ \dot{\boldsymbol{\ell}},\ \mathbf{q},\ \dot{\mathbf{q}},\ \mathbf{p}_1,\ \mathbf{p}_2,\ \mathbf{F}_{net},\ \mathbf{F}_{net,des},\ \dot{\mathbf{F}}_{net,des}) \tag{27}$$

Note that this control law requires feedback of both the position and velocity errors, as well as of the force applied to the platform. The terms $\mathbf{q}$ and $\dot{\mathbf{q}}$ are determined using the direct kinematics. A detailed look shows that the controller is made of two nested loops, a faster internal force loop and a slower external position loop. An advantage is that it does not require an estimate of the piston acceleration or of the derivative of the force, $\dot{\mathbf{F}}_{net}$, which are problematic in the presence of noise. The schematic view of the full model-based force controller diagram for the servomechanism is depicted in Fig. 4.

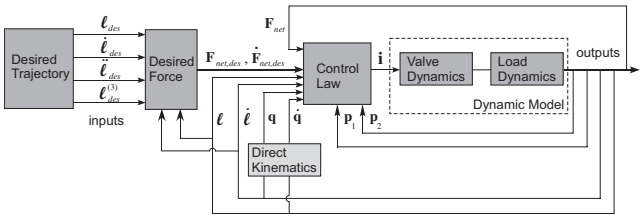


Fig. 4. Schematic view of the full model-based force controller diagram for the 6-dof electrohydraulic Stewart mechanism.

## IV. Simulation Results

The tracking performance of the controller is evaluated next. The system parameters include the platform mass $m = 150\,\mathrm{kg}$, the moments of inertia about the platform center of mass $I_{xx} = I_{yy} = 25\,\mathrm{kgm}^2$, $I_{zz} = 50\,\mathrm{kgm}^2$, and friction parameters, $b_j = 400\ \mathrm{Ns/m}$, $F^*_{C0,j} = 50\ \mathrm{N}$ and $F^*_{s0,j} = 200\ \mathrm{N}$, which were experimentally computed at a single dof servomechanism [23]. The Stewart mechanism is considered as a 6-6 symmetric mechanism. The joints of the movable platform and fixed base lie at equal peripheral distances and at radii $0.5\,\mathrm{m}$ and $1.0\,\mathrm{m}$, respectively, and the joint distances at the movable platform and fixed base are $0.2\,\mathrm{m}$ and $0.3\,\mathrm{m}$, respectively. To compute the matrix control gains, we first require that all dofs are critically damped. Hence, $\zeta_j = 1$, $j=1,...,6$. Next, we require a settling time of about $1\mathrm{s}$, yielding $\omega_j = 2\pi$ rad/s, $j=1,...,6$. Further, the valve parameters have been experimentally computed [23] as, $K_{1,main} = 1.5\times10^{-5}\ \mathrm{m}^{7/2}/(\mathrm{A\,kg}^{1/2})$, $K_{0,main} = 5\times10^{-9}\ (\mathrm{m}^7/\mathrm{kg})^{1/2}$, $K_{0,leak} = 3.5\times10^{-9}\ (\mathrm{m}^7/\mathrm{kg})^{1/2}$, $k_{1,main} = 0$, $k_{2,main} = 6.8\times10^{-3}\,\mathrm{m}^{7/2}/(\mathrm{A}^2\mathrm{kg}^{1/2})$, $k_{1,leak} = -1.32\times10^{-5}\ \mathrm{m}^{7/2}/(\mathrm{A\,kg}^{1/2})$, $k_{2,leak} = 6\times10^{-3}\,\mathrm{m}^{7/2}/(\mathrm{A}^2\,\mathrm{kg}^{1/2})$, $k_{3,leak} = -0.84\,\mathrm{m}^{7/2}/(\mathrm{A}^3\,\mathrm{kg}^{1/2})$, $k_0 = 1.3\times10^{-8}\ (\mathrm{m}^7/\mathrm{kg})^{1/2}$, $i_{0,main} = 1\,\mathrm{mA}$, and $i_{0,leak} = 1.5\,\mathrm{mA}$. All these constants were experimentally computed for a two-land-four-way spool MOOG G761-3004 Series

high-performance servovalve. Further, the hydraulic hose para-meters were experimentally computed [23] as, $I=3.8\times 10^{7}\,\mathrm{kg/m^4}$, $R=6.57\times10^{8}\,\mathrm{Ns/m^5}$, $C=1.072\times10^{-12}\,\mathrm{m^5/N}$. Simulations runs were obtained using a number of desired trajectories. As an example, Fig. 5 shows typical results, in which the desired trajectory is given by,

$$z_0(t)=z_{c1}+z_c\sin(2\pi f t) \tag{28}$$

where $f=0.5\,\mathrm{Hz}$, $z_c=0.1\,\mathrm{m}$ and $z_{c1}=1.34\,\mathrm{m}$.

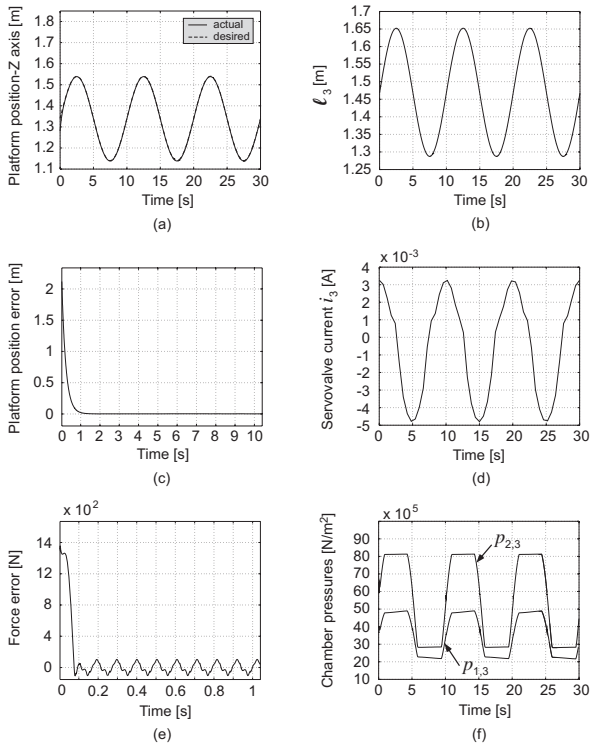


Fig. 5. Simulation results. (a) Platform displacement response, (b) an actuator position, (c) platform position error, (d) control input, (e) actuation force error, and (f), chamber pressure histories of the same actuator.

## V. Conclusions

In this paper, a position tracking controller for a six dof electrohydraulic Stewart platform mechanism using a fast model-based inner force tracking loop was developed. The rigid body equations of motion and the hydraulic dynamics were integrated to form the system dynamics. Friction and leakage of hydraulic elements were included in the full electrohydraulic model. The control analysis was based on a nonlinear input-output linearization control approach. The control law includes a PD part driving the tracking error to zero exponentially. The approach can be further extended to hydraulic manipulator and simulator control.

## References

[1] V. E. Gough, Discussion in London: Automobile Stability, Control, and Tyre Performance, *In Proceedings of the IMechE's Automobile Division*, 1956, pp. 392-394.

[2] The True Origins of Parallel Robots, Available from: <http://www.parallemic.org>.

[3] D. Stewart, "A platform with six degrees of freedom," *In Proceedings of the IMechE*, Vol. 180, Pt. 1, No 15, 1965-66, pp. 371–385.

[4] L-W. Tsai, *Robot Analysis, The Mechanics of Serial and Parallel Manipulators*, J. Wiley & Sons, 1999.

[5] M. J. Liu, C. X. Li, and C. N. Li, "Generalized Stewart-Gough Platforms and Their Direct Kinematics," *IEEE Transactions on Robotics and Automation*, Vol. 16, No. 1, 2000, pp. 94–98.

[6] X. S. Gao, D. Lei, Q. Liao, and G. F. Zhang, "Generalized Stewart-Gough Platforms and Their Direct Kinematics," *IEEE Transactions on Robotics*, Vol. 21, No. 2, 2005, pp. 141–151.

[7] G. Lebret, K. Liu, and F. L. Lewis, "Dynamic Analysis and Control of a Stewart Platform Manipulator," *Journal of Robotic Systems*, Vol. 10 No. 5, 1993, pp. 629–655.

[8] L-W. Tsai, "Solving the Inverse Dynamics of a Stewart-Gough Manipulator by the Principle of Virtual Work," *Journal of Mechanical Design, Transactions of the ASME*, Vol. 122, 2000, pp. 3–9.

[9] H. E. Merritt, *Hydraulic Control Systems*, J. Wiley, 1967.

[10] M. Jelali, and A. Kroll, *Hydraulic Servosystems: Modelling, Identification and Control*, Springer, 2003.

[11] D. Garagic, and K. Srinivasan, "Application of Nonlinear Adaptive Control Techniques to an Electrohydraulic Velocity Servomechanism," *IEEE Trans. on Control Systems Tech.*, Vol. 12, No. 2, 2004, pp. 303–314.

[12] M. R. Sirouspour, and S. E. Salcudean, "Nonlinear Control of Hydraulic Robots," *IEEE Trans. on Robotics and Automation*, Vol. 17, No. 2, 2001, pp. 173–182.

[13] N. Niksefat, and N. Sepehri, "Robust Force Controller Design for an Electro-Hydraulic Actuator Based on Nonlinear Model," *Proc. 1999 IEEE Int. Conf. Robotics & Automation*, San Francisco, pp. 200–206.

[14] R. Liu, and A. Alleyne, "Nonlinear Force/Pressure Tracking of an Electro-Hydraulic Actuator," *Trans. of the ASME*, vol. 122, 2000, pp. 232–237.

[15] A. G. Alleyne, and R. Liu, "Systematic Control of a Class of Nonlinear Systems with Application to Electrohydraulic Cylinder Pressure Control," *IEEE Trans. on Control Systems Tech.*, vol. 8, No. 4, 2000, pp. 623–634.

[16] G. A. Sohl, and J. E. Bobrow, "Experiments and Simulations on the Nonlinear Control of a Hydraulic Servosystem," *IEEE Trans. on Control Systems Tech.*, vol. 7, No. 2, 1999, pp. 238–247.

[17] M. Honegger, and P. Corke, "Model-Based Control of Hydraulic Actuated Manipulators," *Proc. 2001 IEEE Int. Conf. on Robotics & Automation*, Seoul, Korea, pp. 2553–2559.

[18] I. Davliakos, and E. Papadopoulos**,** "Development of a Model-Based Nested Controller for Electrohydraulic Servos," *Proc.13th IEEE Mediterranean Conference on Control and Automation*, June 27-29, 2005, Limassol, Cyprus

[19] D. Rowell, and D. N. Wormley, *System Dynamics: An Introduction*, Prentice Hall, 1997.

[20] J. F. Blackburn, G. Reethof, and J. L. Shearer, *Fluid Power Control*, Cambridge, MA: MIT Press, 1960.

[21] W. J. Thayer, *Specification Standards for Electrohydraulic Flow Control Servovalves*, Technical Bulletin 117, Moog Incorporation Control Division, E. Aurora, New York, 1962.

[22] R. Rosenberg, and D. Karnopp, *Introduction to Physical System Dynamics*, McGraw Hill, New York, 1983.

[23] I. Davliakos, A. Zafiris, and E. Papadopoulos, "Joint Space Controller Design for Electrohydraulic Servos," *Proc. 2006 IEEE Int. Symp. on Computer-Aided Control Systems Design*, *(CACSD '06)*, October 4-6, 2006, Tech. Universität München, Munich, Germany, pp. 796-801.